Molecular Therapy
Methods & Clinical Development
Original Article

Intracranial delivery of AAV9 gene therapy partially prevents retinal degeneration and visual deficits in CLN6-Batten disease mice

Katherine A. White,[1,10] Hemanth R. Nelvagal,[2,5,10] Timothy A. Poole,[2] Bin Lu,[3] Tyler B. Johnson,[1,4] Samantha Davis,[1] Melissa A. Pratt,[1] Jon Brudvig,[1] Ana B. Assis,[5] Shibi Likhite,[6] Kathrin Meyer,[7,9] Brian K. Kaspar,[7,9] Jonathan D. Cooper,[2,5,11] Shaomei Wang,[3,11] and Jill M. Weimer[1,4,8,11]

[1]Pediatrics and Rare Diseases Group, Sanford Research, Sioux Falls, SD 57104, USA; [2]Pediatric Storage Disorders Laboratory, Division of Genetics and Genomics, Department of Pediatrics, Washington University School of Medicine, St. Louis, MO 63110, USA; [3]Regenerative Medicine Institute, Cedars-Sinai Medical Center, Los Angeles, CA 90048, USA; [4]Amicus Therapeutics, Philadelphia, PA 19104, USA; [5]Department of Pediatrics, The Lundquist Institute at Harbor-UCLA Medical Center and David Geffen School of Medicine, UCLA, Torrance, CA 90502, USA; [6]Nationwide Children's Hospital. He was involved in AAV9 construct development; [7]The Research Institute at Nationwide Children's Hospital, Columbus, OH 43205, USA; [8]Department of Pediatrics, Sanford School of Medicine, University of South Dakota, Sioux Falls, SD 57069, USA; [9]Department of Pediatrics, The Ohio State University, Columbus, OH 43210, USA

Batten disease is a family of rare, fatal, neuropediatric diseases presenting with memory/learning decline, blindness, and loss of motor function. Recently, we reported the use of an AAV9-mediated gene therapy that prevents disease progression in a mouse model of CLN6-Batten disease (*Cln6*^{nclf}), restoring lifespans in treated animals. Despite the success of our viral-mediated gene therapy, the dosing strategy was optimized for delivery to the brain parenchyma and may limit the therapeutic potential to other disease-relevant tissues, such as the eye. Here, we examine whether cerebrospinal fluid (CSF) delivery of scAAV9.CB.CLN6 is sufficient to ameliorate visual deficits in *Cln6*^{nclf} mice. We show that intracerebroventricular (i.c.v.) delivery of scAAV9.CB.CLN6 completely prevents hallmark Batten disease pathology in the visual processing centers of the brain, preserving neurons of the superior colliculus, thalamus, and cerebral cortex. Importantly, i.c.v.-delivered scAAV9.CB.CLN6 also expresses in many cells throughout the central retina, preserving many photoreceptors typically lost in *Cln6*^{nclf} mice. Lastly, scAAV9.CB.CLN6 treatment partially preserved visual acuity in *Cln6*^{nclf} mice as measured by optokinetic response. Taken together, we report the first instance of CSF-delivered viral gene reaching and rescuing pathology in both the brain parenchyma and retinal neurons, thereby partially slowing visual deterioration.

INTRODUCTION

Batten disease (neuronal ceroid lipofuscinosis [NCL]) is a family of rare, fatal, neuropediatric lysosomal storage disorders, typically presenting in early childhood with memory/learning decline, blindness, and loss of motor function.[1,2] Each of these disorders is caused by mutations in one of thirteen different genes, which encode a variety of soluble and transmembrane NCL proteins.[3] While the function of these NCL proteins is not entirely understood, some have been implicated in intracellular trafficking, endocytosis, and lysosomal maintenance, among other cellular functions, and therapeutic approaches for transmembrane variants are complicated by the inability to cross-correct neighboring cells.[4] At the cellular level, Batten disease primarily affects the central nervous system (CNS), where lysosomes accumulate abundant lipofuscin, a chronic neuroimmune response develops, and neurons progressively perish.[5] While no cure exists for any form of Batten disease, enzyme replacement therapy (ERT) effectively slows progression for some patients of the secreted CLN2 sub-form (ClinicalTrials.gov: NCT01907087),[6,7] and recent clinical trials have focused on ERTs, small molecule therapies, stem cell therapy, and gene therapy.[5]

Gene therapy is an attractive strategy for disorders such as Batten disease, where the function of the disease protein is unknown. We and others recently characterized the utility of a single, intracerebroventricular (i.c.v.) injection of a self-complementary (sc) adeno-associated virus serotype 9 (AAV9) gene therapy in a mouse model of variant late infantile CLN6-Batten disease (CLN6 disease), a variant where patients have biallelic mutations in the *CLN6* gene and loss of the transmembrane protein and present with symptoms in childhood.[8,9] Using a *Cln6*^{nclf} mouse model, it was demonstrated that early treatment with cerebrospinal fluid (CSF)-mediated delivery of

Received 27 April 2020; accepted 31 December 2020;
https://doi.org/10.1016/j.omtm.2020.12.014.

[10]These authors contributed equally

[11]These authors contributed equally

Correspondence: Shaomei Wang, Regenerative Medicine Institute, Cedars-Sinai Medical Center, 8700 Beverly Blvd, Los Angeles, CA 90048, USA
E-mail: shaomei.wang@cshs.org
Correspondence: Jill M. Weimer, Pediatrics and Rare Diseases Group, Sanford Research, 2301 E 60th St. N, Sioux Falls, SD 57104, USA.
E-mail: jill.weimer@sanfordhealth.org

scAAV9 resulted in near complete prevention of motor, memory/learning, and survival deficits[8]. With these preclinical data, a phase I/II clinical trial was initiated in 2016 (ClinicalTrials.gov: NCT02725580). Importantly, interim outcome data reported in late 2019 showed stabilization of motor, language, and visual function, along with a favorable safety profile.[10]

While our viral-mediated gene therapy for CLN6 disease appears successful, the i.c.v. dosing strategy used in our previous study was optimized for neuronal delivery in the brain parenchyma and may limit the therapeutic potential to other Batten disease-relevant tissues such as the eye. As Batten disease patients experience a severe decline in quality of life as they lose vision and become blind, effective treatments must target critical structures not only in the brain and spinal cord but also in the retina. Construct targeting and distribution are highly dependent on the viral vector and serotype, delivery route, and dosing characteristics (i.e., timing, size, and purity), requiring careful consideration to yield the most effective transduction of the most vulnerable cells.[11–14] Gene therapies focused on the eye, such as the US Food and Drug Administration (FDA)-approved Luxturna (voretigene neparvovec), have generally relied on direct delivery routes that are most effective in reaching the retina, such as subretinal or intravitreous delivery routes.[13,15] Unfortunately, while these routes reach the retina, they have limited penetrance to the brain. For multi-organ diseases such as Batten disease, eye-specific routes of administration would require multiple vectors to be dosed, at minimum, in parallel to the brain parenchyma, increasing the potential for toxicity, immune reaction, and other side effects. While more systemic delivery methods, such as intravenous delivery, have been shown to reach both the eye and brain with a single dose, they require significantly larger doses than other targeted approaches and have been linked to acute hepato-toxicity and other side effects.[16–18]

Here, we sought to determine whether a single i.c.v. injection with an AAV9 gene therapy construct is sufficient to target and prevent the onset of pathology in both the eye and visual centers of the brain in a mouse model of variant late infantile CLN6 disease. *Cln6*^{nclf} mice were treated at postnatal day 1 (P1) with either PBS or scAAV9.CB.CLN6. This single CSF-administered dose prevented Batten disease-associated pathology in visual centers of the brain, expressed in the retina and largely prevented central photoreceptor loss, and partially preserved visual acuity in *Cln6*^{nclf} mice. As such, a single, i.c.v.-mediated administration of scAAV9 is able to express in the retina and preserve intermediate visual function in addition to its effects in the brain, which will help optimize gene therapies for CLN6 disease and other neurodegenerative diseases affecting the retina in the future.

RESULTS

i.c.v. delivery of AAV9-CLN6 prevents Batten disease pathology in visual centers of the brain

Wild-type and *Cln6*^{nclf} mice were dosed with scAAV9.CB.CLN6 (5×10^{10} viral genomes (vg)/animal, 4 μL volume in phosphate-buffered saline (PBS)) or PBS (4 μL volume) at P1 via i.c.v. injection as previously described.[8] The AAV9 serotype was chosen to preferentially target neurons at high efficiency when paired with a hybrid chicken-β-actin (CB) promoter and has previously been shown to achieve widespread expression of the human CLN6 protein in the mouse brain.[8] Since loss of visual function is a key feature of CLN6 disease, and visual function relies on both the eye and the brain, we first asked whether a single i.c.v. injection of scAAV9.CB.CLN6 impacted Batten disease pathology in visual centers of the brain.

Thalamocortical visual pathways including the dorsal lateral geniculate (DLG) and primary visual cortex (V1) are typically considered to be key visual pathways in humans and are primarily responsible for the processing of signals from cone-rich retinal regions with high visual acuity (i.e., the fovea).[19] Other areas, such as the superior colliculus (SC), primarily process signals from rod-rich regions located in the retinal periphery and are important for the detection of movement; in mice, the SC receives projections from 85%–90% of retinal ganglion cells (RGCs).[20,21] Therefore, we analyzed pathology within the DLG, V1, and SC to investigate two parallel visual information streams in *Cln6*^{nclf} mice.

The accumulation of fluorescent lipofuscin within lysosomes is a cellular signature of Batten disease.[5] While the precise impact of this storage material on disease progression is unknown, its accumulation is often used as a correlate for disease burden.[8] Here, we show pronounced autofluorescent storage material (ASM) accumulation in *Cln6*^{nclf} animals in all of the central visual centers of the brain (DLG, V1, SC), with neonatal scAAV9.CB.CLN6 treatment preventing this characteristic accumulation at all time points examined (Figure 1). Collectively, Batten disease is also characterized by a pronounced and early neuroimmune response in astrocytes and microglia, as evidenced by increases in glial fibrillary acidic protein (GFAP) and cluster of differentiation 68 (CD68) immunoreactivity.[5] Similar to ASM accumulation, *Cln6*^{nclf} animals presented with robust astrocyte ($GFAP^+$) and microglial ($CD68^+$) immunoreactivity in all visual centers examined, with scAAV9.CB.CLN6 treatment preventing this response at all time points examined (Figures 2 and 3, respectively). Lastly, as CLN6 disease is a neurodegenerative disorder, we asked whether scAAV9.CB.CLN6 treatment prevented the loss of neurons in these critical visual centers. Using unbiased stereological counts on Nissl-stained sections, scAAV9.CB.CLN6 prevented the loss of neurons in all visual centers examined, at all time points examined (Figure 4). These results show scAAV9.CB.CLN6's robust ability to prevent pathology in visual centers of the brain and, importantly, shed light on hallmark Batten disease pathology in the SC that has not previously been characterized in detail for this form of NCL, despite its presence even at early time points (3 months of age).

i.c.v.-delivered AAV9 expresses in the eye, preserving photoreceptors in *Cln6*^{nclf} mice

As neuronal integrity was preserved in the visual processing centers of the brain in AAV9-treated *Cln6*^{nclf} mice, we next examined neuronal integrity in the retina to see if this pathology had also been prevented. Untreated *Cln6*^{nclf} mice progressively lost photoreceptors from 3 to 9 months of age (Figures 5A–5C, arrows). In contrast, representative

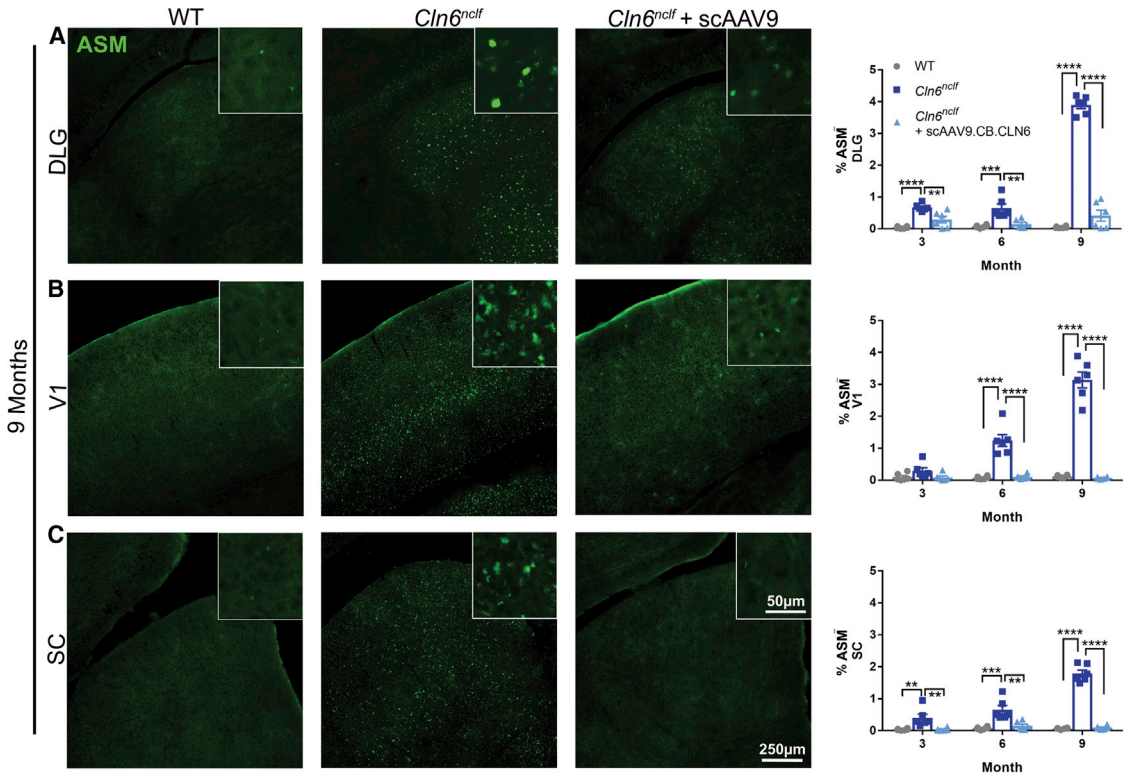

Figure 1. CSF delivery of scAAV9.CB.CLN6 prevents classic autofluorescent storage material accumulation in several visual processing centers of the brain in *Cln6*^{nclf} mice

(A–C) A single, postnatal day 1 injection of scAAV9.CB.CLN6 delivered via CSF prevents storage material accumulation (ASM, green) in the (A) dorsal lateral geniculate (DLG), (B) primary visual cortex (V1), and (C) superior colliculus (SC) until 9 months of age. n = 6/treatment for each time point, represented by equal numbers of males and females. Mean ± SEM, one-way ANOVA for each time point, Bonferroni correction. **p < 0.01, ***p < 0.001, ****p < 0.0001.

images of wild-type animals show 10–12 layers of photoreceptors at each time point examined, with scAAV9.CB.CLN6 partially preserving these layers in the central retina of *Cln6*^{nclf} mice until 9 months of age (Figures 5A–5F). However, photoreceptors in the peripheral retina continued to be lost following scAAV9.CB.CLN6 treatment with age, beginning at 3 months of age to 9 months of age (Figures 5D–5F).

Given the unexpected degree of photoreceptor protection in the central retina of *Cln6*^{nclf} mice treated with an i.c.v. injection of scAAV9.CB.CLN6, we asked whether human CLN6 was present in the retina of treated mice. To characterize the expression patterns of i.c.v.-delivered scAAV9.CB.CLN6 in the retina, we visualized endogenous mouse *Cln6* transcript (*mCln6*) and transgenic human *CLN6* (*hCLN6*) transcript with a modified *in situ* technique (RNAscope), as well as hCLN6 protein via immunostaining. A lack of commercial antibodies targeting mouse Cln6 precluded dual immunolabeling. While endogenous *mCln6* transcript was present primarily in the inner and outer nuclear layers, with lower-level expression in RGCs and the retinal pigmented epithelium (RPE) (Figure 6A), *hCLN6* transcript and protein was expressed widely throughout the RGC layer, inner nuclear layer, outer nuclear layer, RPE, and choroid, with particularly robust expression in RGCs (Figures 6B and 6D–6G; Figure S1). Additionally, hCLN6 immunoreactivity was predominantly present in the central retina, with reduced expression in the middle and peripheral areas (Figure 6C; Figure S2). When co-labeled with a marker for photoreceptor outer segments (Rhodopsin [Rho]$^{+}$), RGCs (BRN3a^{+}), bipolar cells (PKCa^{+}), and Müller glia (glutamine synthetase [GS^{+}]), hCLN6 immunolabeling again colocalized primarily with RGCs (Figures 6D–6G), consistent with retinal layer distribution and previous reports of predominantly neuronal expression following subretinal delivery of AAV9.[22] Taken together, a single i.c.v. injection of scAAV9.CB.CLN6 expresses in the retina and

Table 1. Optokinetic tracking sample sizes

	Wild type (n)		*Cln6*^{nclf} (n)		*Cln6*^{nclf} + scAAV9 (n)	
	Male	Female	Male	Female	Male	Female
3 months	10	13	13	17	17	11
6 months	7	10	10	12	14	8
9 months	3	3	6	4	11	6

Related to Figure 7.

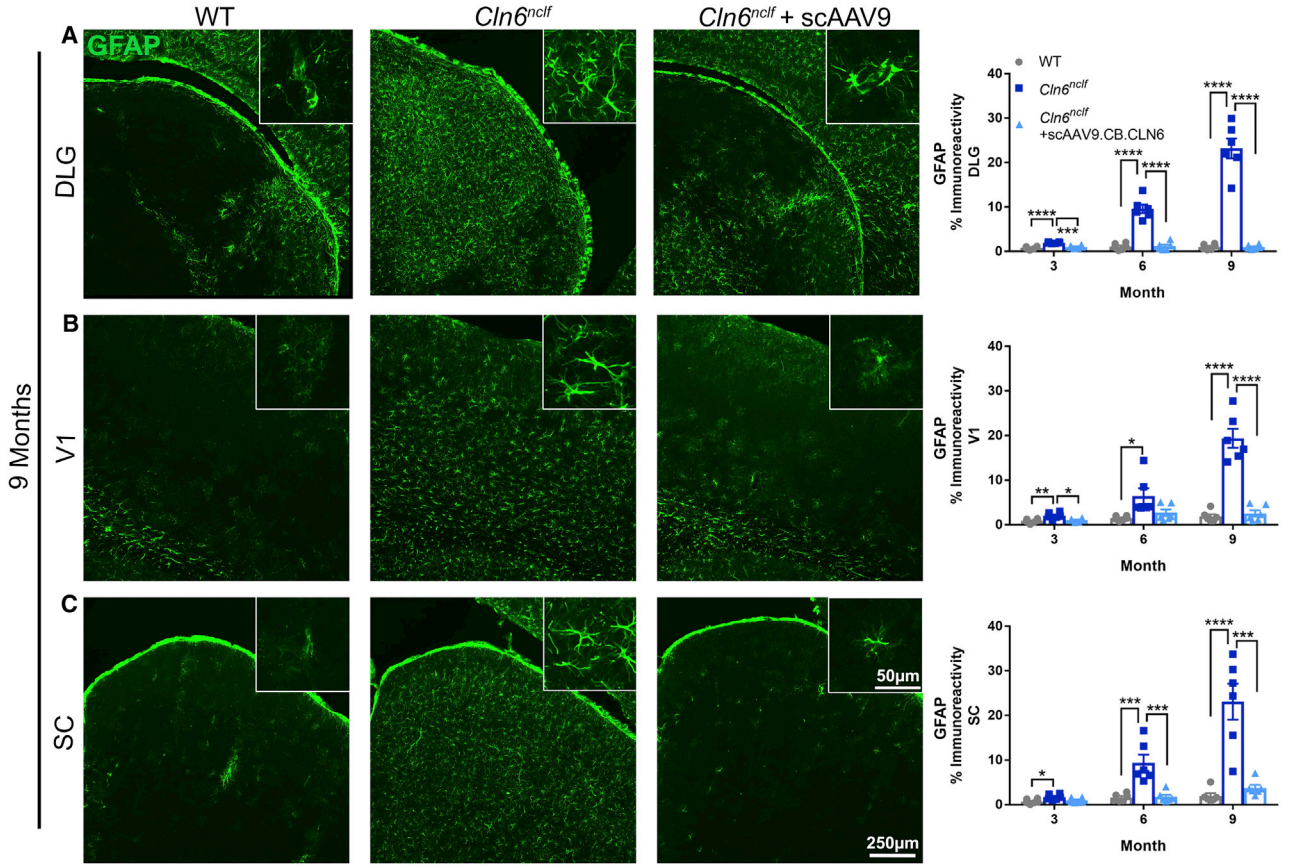

Figure 2. CSF delivery of scAAV9.CB.CLN6 prevents increased astrocyte reactivity in the DLG, V1, and SC

(A–C) A single, postnatal day 1 injection of scAAV9.CB.CLN6 delivered via CSF prevents GFAP^{+} astrocyte reactivity (green) in the (A) DLG, (B) V1, and (C) SC until 9 months of age. n = 6/treatment for each time point, represented by equal numbers of males and females. Mean ± SEM, one-way ANOVA for each time point, Bonferroni correction. *p < 0.05, **p < 0.01, ***p < 0.001, ****p < 0.0001.

significantly preserves central retinal photoreceptors in *Cln6*^{nclf} mice, despite expression patterns that differ somewhat from endogenous patterns.

i.c.v.-delivered AAV9 significantly preserves visual acuity in *Cln6*^{nclf} mice

To assess whether the preservation of retinal and other visual pathway neurons rescued visual function, animals were tested for visual acuity using optokinetic response from 3 to 9 months of age (OptoMotry, Cerebral Mechanics) (Figure 7A). Briefly, animals were individually placed on a platform surrounded by four monitors arranged in a square, and a gradient of varying contrasts rotated around the mice in either a clockwise or counterclockwise fashion. To assess visual acuity, an experimenter blinded to genotype and treatment status observed the animal and determined whether the animal was tracking the gradient. Beginning at 6 months of age, untreated *Cln6*^{nclf} animals of both sexes declined in spatial visual acuity (cycles/degree), with deficits progressing until the last time point at 9 months of age (Figures 7B and 7C). At 6 and 9 months, scAAV9.CB.CLN6-treated *Cln6*^{nclf} mice maintained visual acuity intermediate of untreated *Cln6*^{nclf} mice and wild-type mice, especially in female mice, indicating some therapeutic value of i.c.v.-delivered gene therapy on visual function. Importantly, untreated female *Cln6*^{nclf} mice had a significantly steeper decline in vision over the 6-month period when compared to either female scAAV9.CB.CLN6-treated *Cln6*^{nclf} or wild-type control mice (Figure 7C, comparison of slope), again supporting a therapeutic effect of i.c.v.-delivered scAAV9.CB.CLN6 on visual function.

DISCUSSION

In this study we show marked preservation of neurons in both the central retina and central visual pathways of the brain resulting from a single i.c.v. dose of scAAV9.CB.CLN6 to *Cln6*^{nclf} mice. i.c.v. delivery led to efficient expression of CLN6 throughout many retinal layers, preserving a significant proportion of central retinal photoreceptors and partial visual function in treated *Cln6*^{nclf} mice until the last time point examined. Taken together, these data suggest that i.c.v. delivery of scAAV9.CB.CLN6 effectively protects central visual neurons within the brain and expresses in the retina, resulting in the partial prevention of retinal pathology and amelioration of visual decline.

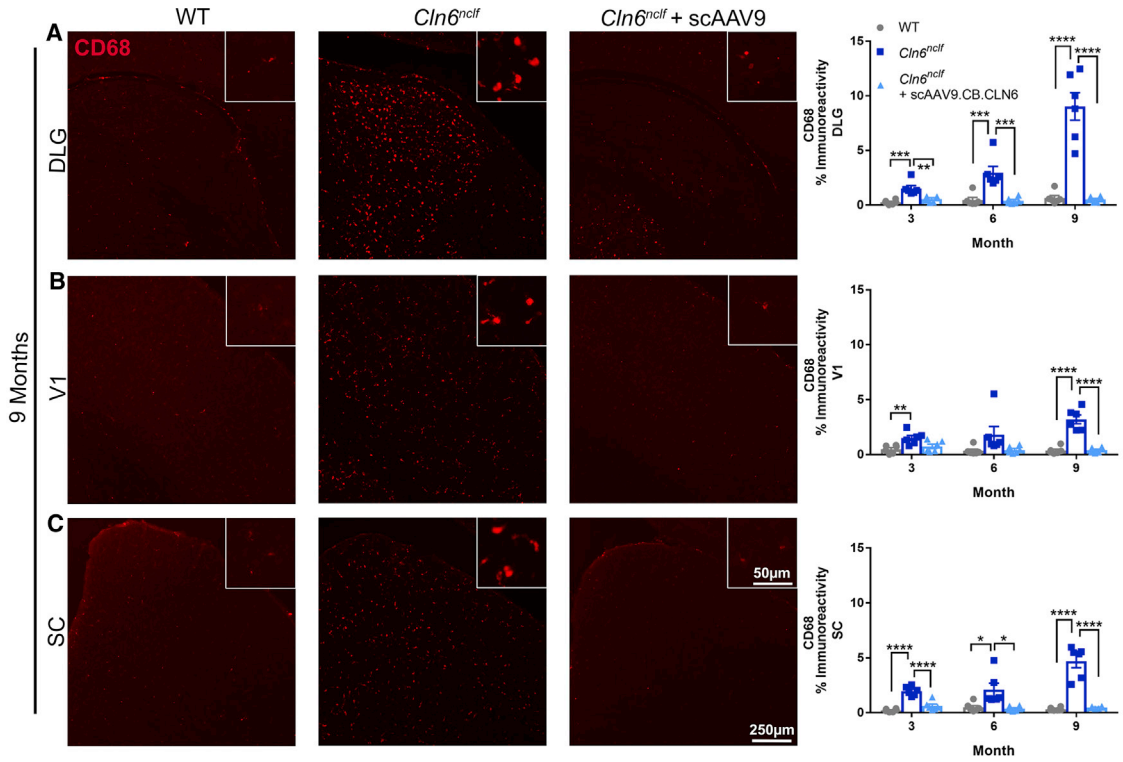

Figure 3. CSF delivery of scAAV9.CB.CLN6 prevents microglial activation in visual processing centers of the brain

(A–C) A single, postnatal day 1 injection of scAAV9.CB.CLN6 delivered via CSF prevents CD68^{+} microglial activation (red) in the (A) DLG, (B) V1, and (C) SC until 9 months of age. n = 6/treatment for each time point, represented by equal numbers of males and females. Mean ± SEM, one-way ANOVA for each time point, Bonferroni correction. *p < 0.05, **p < 0.01, ***p < 0.001, ****p < 0.0001.

Thalamocortical visual pathway pathology is well established in multiple forms of Batten disease including CLN6 and, together with retinal pathology, has been considered a correlate of the visual failure evident in many forms of Batten disease.[20,24–26] Indeed, in mouse models of CLN3-Batten disease, pathology is present in the visual thalamocortical system at 6 months of age despite a lack of retinal neurodegeneration, suggesting a central thalamocortical cause of visual failure in CLN3 disease mice that perhaps precedes progressive photoreceptor loss in the retina.[20] Until now, the potential involvement of other retinorecipient nuclei has been overlooked in CLN6 disease.

Our data from untreated *Cln6^{nclf}* mice reveal for the first time progressive neuron loss, ASM accumulation, and glial activation in the SC, a crucial visual center in mammals that, in mice, receives projections from up to 90% of RGCs.[21] i.c.v. delivery of scAAV9.CB.CLN6 effectively prevented pathology in this region, in addition to previously identified pathology in the visual thalamocortical system (DLG, V1).[26] As these phenotypes were apparent early in *Cln6^{nclf}* disease progression (3 months of age), these data are additionally indicative of the severity of disease in the SC and its importance in the visual pathway of mice. These results are consistent with the therapeutic effects of i.c.v. delivery of scAAV9.CB.CLN6 on the somatosensory thalamocortical system, but the unanticipated beneficial impact of this treatment upon retinal pathology and visual acuity suggests this i.c.v. route of administration could potentially provide some benefit for retinal manifestations of CLN6 disease in lieu of adjunctive injections directly treating the eye.[8]

While directing gene therapy to the CSF is a logical approach for treating brain manifestations of disease, it has always been considered unlikely to exert any therapeutic effect upon the retina, as CSF does not directly contact ocular structures other than the optic nerve.[27] Indeed, prior progress in treating visual manifestations of Batten disease have relied primarily upon intravitreal delivery of gene, enzyme replacement, or cellular therapies with varying degrees of success.[28–31] However, our data reveal that i.c.v.-delivered scAAV9.CB.CLN6 not only provides hCLN6 expression in the *Cln6^{nclf}* retina but also partially rescues retinal pathology, although with the current paradigm this is predominantly confined to the central retina.

It is not clear why such robust pathological rescue in our study did not lead to full functional rescue in treated *Cln6^{nclf}* mice. Although our approach preserved central retina photoreceptors, peripheral photoreceptors in i.c.v.-treated *Cln6^{nclf}* mice continued to degenerate with age, and this process may have impacted visual acuity in older AAV9-treated *Cln6^{nclf}* mice. Previous attempts at retinal gene therapy

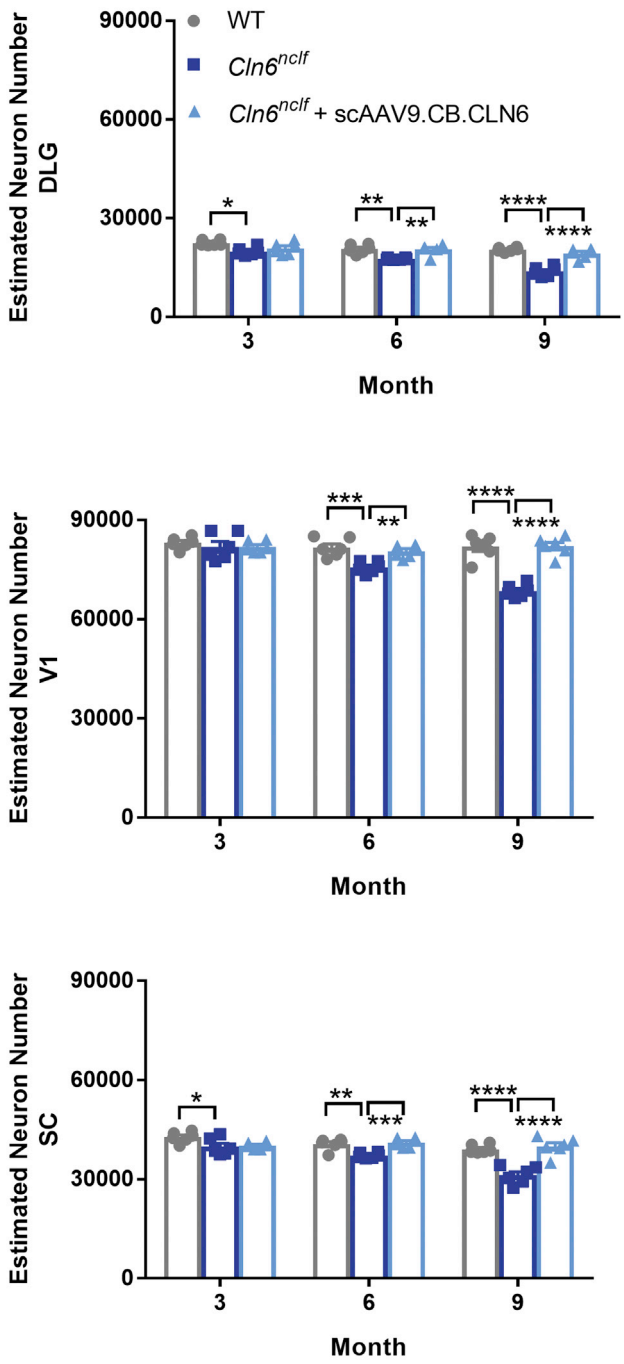

Figure 4. i.c.v. delivery of scAAV9.CB.CLN6 prevents neuronal loss in the DLG, V1, and SC

(A–C) A single, postnatal day 1 injection of scAAV9.CB.CLN6 delivered via CSF prevents progressive neuronal loss in the (A) DLG, (B) SC, and (C) V1 until 9 months of age. n = 6/treatment for each time point, represented by equal numbers of males and females. Mean ± SEM, one-way ANOVA for each time point, Bonferroni correction. *p < 0.05, **p < 0.01, ***p < 0.001, ****p < 0.0001.

in NCL mice have suggested transducing bipolar cells to be important for preserving photoreceptors and visual function.[28,32] In contrast, in this study *hCLN6* expression was mainly observed in the RGC and photoreceptor layers, with little evidence of bipolar cell expression, yet this expression pattern preserved considerable numbers of central photoreceptors and resulted in partial maintenance of visual function. Therefore, it is possible that both RGCs and bipolar cells have important roles to play in preserving photoreceptor function in *Cln6*^{nclf} mice. Additionally, there could be opportunities for improving *hCLN6* expression in cell types that show low levels of expression in the current study, as there is considerable evidence that AAV9 transduction is more widespread than its product's transcript or protein expression.[33,34]

It is also important to note that this study concluded at 9 months of age and only assessed visual function via optokinetic tracking and not electroretinography, in which the latter technique gives a more complete and precise picture of the function of the entire retina. Therefore, while our study shows partial preservation of visual function in AAV9-treated *Cln6*^{nclf} mice, it is possible that a more thorough longitudinal analysis would point to additional aspects of visual function that can be improved. Nonetheless, our i.c.v.-treated *Cln6*^{nclf} mice did not show any signs of retinal toxicity, as have been reported following subretinal delivery of various AAV vectors in mice and non-human primates, suggesting that AAV9 did not adversely affect visual acuity through cell death in this study.[35–37]

There are limited data available regarding retinal transduction via AAV following i.c.v. injection. In the Batten disease field, Katz and colleagues[38] treated *CLN2* mutant canines with AAV2 via i.c.v. injection, delaying disease progression and improving survival with the expression of canine CLN2. However, no expression was observed in the retina of these animals, which suffered from vision loss regardless of pathological improvements in visual centers of the brain. This may be due to the viral subtype used (AAV2 versus AAV9), animal species (canine versus murine), or timing of treatment (3 months of age versus P1), and it is unclear what parameters are necessary for successful retinal expression via CSF delivery, including interactions between capsid and promoter.[39] Importantly, given the differences between visual processes of rodents and humans, our study will need to be validated in animal models that are more reliant on the thalamus for visual processing.

Our study also does not experimentally explain how CSF-delivered AAV9 expresses in distantly located cells in the retina. One potential explanation is that axons of RGCs, which travel from the retina to visual centers of the brain via the optic nerve, may facilitate retrograde axonal transport of viral particles to cell bodies in the retina. AAV9 is known to undergo long-distance retrograde transport in CNS neurons, and it readily transduces RGCs.[40–42] More difficult to explain, however, is the expression of hCLN6 in other retinal cell classes that do not project to the brain. While anterograde transsynaptic transport of AAV and subsequent products has been described following intravitreal injection,[29,43] including the recent report of

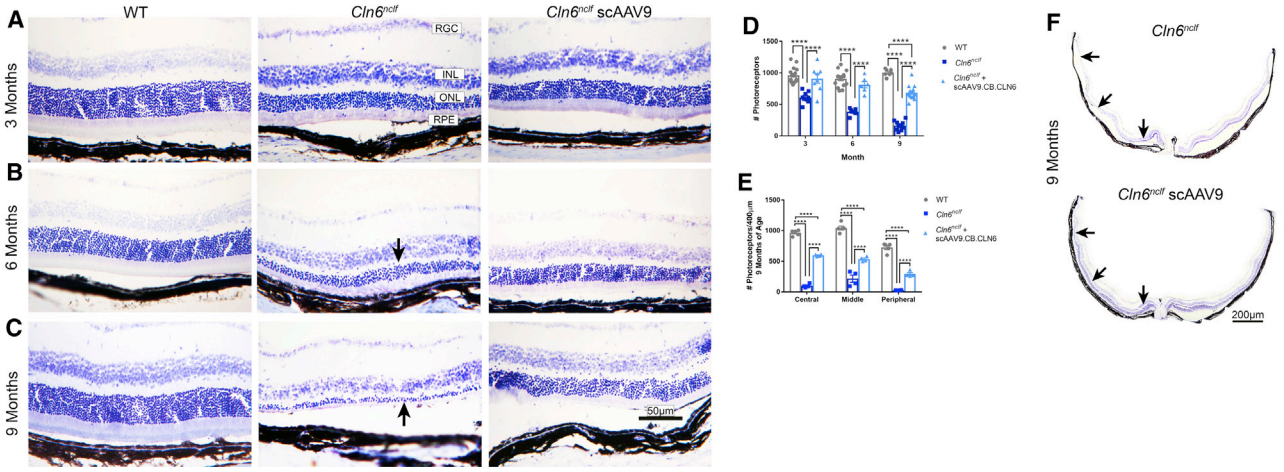

Figure 5. i.c.v. delivery of scAAV9.CB.CLN6 preserves photoreceptors in *Cln6*^{nclf} mice

Retinal sections through the optic nerve head stained with cresyl violet show retinal lamination and photoreceptors. (A–C) A single, postnatal day 1 injection of scAAV9.CB.CLN6 delivered via CSF largely prevents progressive photoreceptor loss in (A) 3 month, (B) 6 month, and (C) 9 month *Cln6*^{nclf} mice (ONL, arrows). As observed from representative images, wild-type animals show 10–12 rows of photoreceptor nuclei, while untreated *Cln6*^{nclf} mice retain only one layer of photoreceptors by 9 months of age. In contrast, AAV9-treated *Cln6*^{nclf} mice maintain 7–8 rows of photoreceptors at all time points examined. (D and E) Quantification of photoreceptor density at different time points is presented in (D), and quantification of photoreceptor density in different retinal areas at 9 months of age is presented in (E). (F) Lastly, retinal montage images through the optic nerve head show severe photoreceptor loss across the whole retina in untreated *Cln6*^{nclf} mice at 9 months of age (arrows), while AAV9 treatment substantially preserves photoreceptors across the central retina at the same age (arrows). Peripheral photoreceptors in treated *Cln6*^{nclf} mice are not preserved at 9 months of age (arrow). Abbreviations: RGC, retinal ganglion cells; INL, inner nuclear layer; ONL, outer nuclear layer; RPE, retinal pigment epithelium. n = 6/treatment for each time point, represented by equal numbers of males and females. Mean ± SEM, two-way ANOVA, Tukey correction. ****$p < 0.0001$.

potential contralateral transfer between eyes in a human gene therapy trial,[44] retrograde transsynaptic transport has not been described, and other retinal cell classes lack CSF-contacting projections. Lastly, while the presence of *hCLN6* mRNA in our study suggests transsynaptic or bulk CSF transportation, additional experiments will be required to elucidate the mechanism of widespread retinal expression following CSF delivery of AAV9.

Regardless of the mechanistic details, the demonstration of any impact upon retinal structure and function in *Cln6*^{nclf} mice following i.c.v. delivery of scAAV9.CB.CLN6 is encouraging from a therapeutic standpoint. Future studies should determine if i.c.v. dosing strategies can be optimized to maintain peripheral photoreceptor integrity and full visual acuity and whether delayed dosing strategies can provide similar benefits. Increased doses, alternative viral serotypes, or combined routes of administration may be necessary to offer the most complete photoreceptor and visual preservation. Taken together, this first report of CSF-mediated AAV9 delivery to the retina has therapeutic promise and will help determine optimal viral dosing strategies for CLN6 disease and other similar neurodegenerative diseases in the future.

MATERIALS AND METHODS

Ethics statement/animals

Mice were maintained on a C57BL/6J background and housed under identical conditions. *Cln6*^{nclf} animals (The Jackson Laboratory, #003605) had an additional cysteine in exon 4 of the *Cln6* gene, resulting in a frameshift mutation and premature stop codon as previously described.[26] Wild-type animals lacked this mutation. All animal studies were conducted in an AAALAC (Association for Assessment and Accreditation of Laboratory Animal Care International)-accredited facility under National Institutes of Health (NIH) guidelines and approved by Sanford Institutional Animal Care and Use Committee (IACUC; United United States Department of Agriculture license 46-R-0009).

i.c.v. injection of either scAAV9.CB.CLN6 (5×10^{10} vg/animal, 4 μL volume in PBS) or PBS (4 μL volume) was performed on P1 as previously described.[8] The injection method and timing were selected to target specific neuronal populations that are relevant in CLN6 Batten disease patients. Animals were sedated via hypothermia during the procedure, monitored until fully recovered, and genotyped as previously described.[26]

Tissue analyses

Animals were sacrificed at 3, 6, or 9 months of age via CO_2 euthanasia and transcardial perfusion with PBS (n = 3/sex/treatment group for each time point). Brains were removed and bisected along the midline into left and right hemispheres. One hemisphere was placed in 4% paraformaldehyde for 24 h followed by transferring to 30% sucrose solution overnight for cryoprotection, while the second hemisphere was bisected again for flash freezing and tissue banking. Eyes were also removed, cornea punctured, and fixed in 4% paraformaldehyde for 1 h. Eyes were sunk in a sucrose gradient, beginning at 10% sucrose solution for 1 h, 20% sucrose solution for 1 h, and lastly 30% sucrose solution overnight.

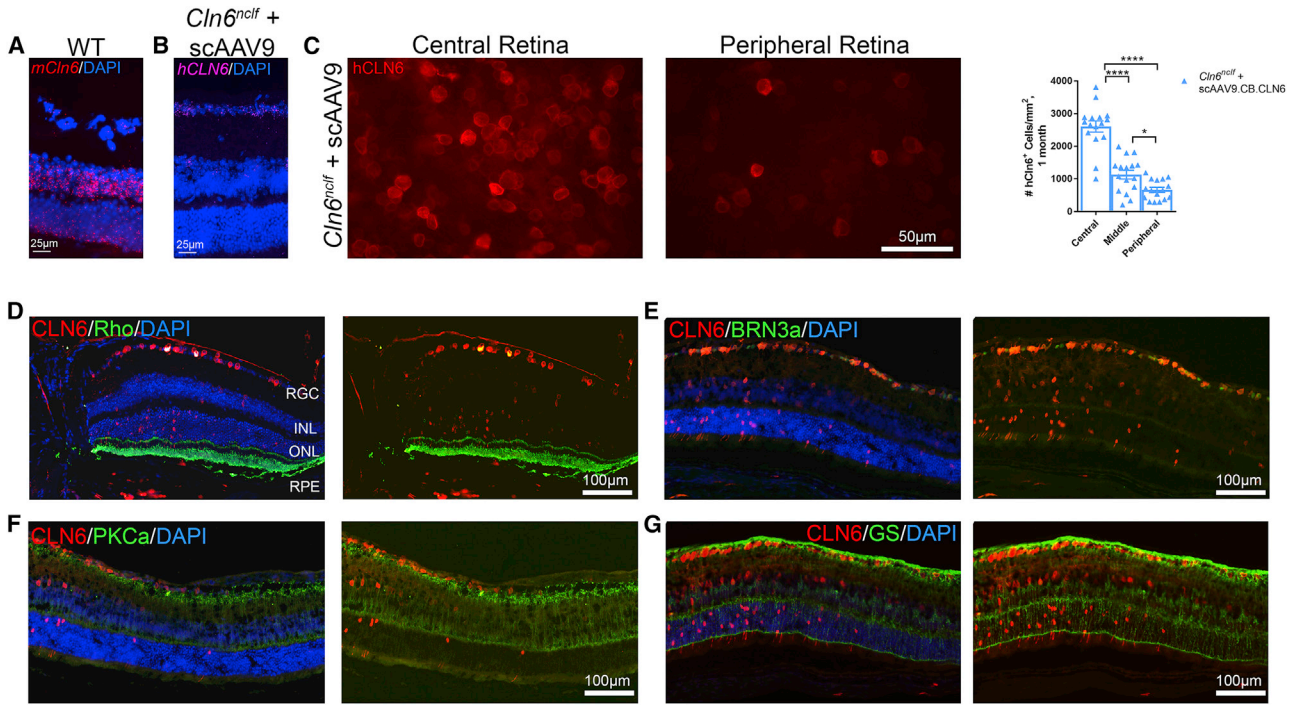

Figure 6. i.c.v. delivery of scAAV9.CB.CLN6 expresses throughout the retinal layers, enabling the local translation of hCLN6 in *Cln6*^{ncl1} mouse retinas

(A and B) Endogenous mouse *Cln6* (*mCln6*) expression in a wild-type animal as detected by RNAscope (A) localized primarily to the inner and outer nuclear layers, showing a different expression pattern as compared to the human *CLN6* (*hCLN6*) transgene (B). (C) Retinal whole-mounts immunolabeled with anti-human CLN6 (red) antibodies detected hCLN6 primarily in the central retina. Quantification is also shown in (C). (D–F) AAV9-treated *Cln6*^{ncl1} mice immunolabeled with anti-human CLN6 (red) and rhodopsin (photoreceptor outer segments, green; D), BRN3a (retinal ganglion cells, green; E), PKCa (rod bipolar cells, green; F), or anti-glutamine synthetase (Müller glia, green; G), show hCLN6 colocalization primarily in RGCs, and also in the INL, ONL, RPE, and choroid. This indicates scAAV9.CB.CLN6 preferentially targeted RGC, INL, ONL, and epithelial layers using this dosing strategy. n = 6/treatment for each time point, represented by equal numbers of males and females. Mean ± SEM, One-way ANOVA, Tukey post-hoc. *p<0.05, ****p<0.0001.

4% paraformaldehyde fixed and cryoprotected brains were sectioned using a Microm H430 freezing microtome (Microm International, Walldorf, Germany) with a Physitemp BFS 40MOA freezing stage (Physitemp Instruments, Clifton, NJ, USA) to obtain 40 μm thick coronal sections. A 1 in 6 series of sections was then selected for analysis of ASM, staining for Nissl substance with cresyl fast violet, and immunohistochemistry, respectively.

Cresyl fast violet staining

Sections were stained for cresyl fast violet as previously described.[45,46] Briefly, a 1 in 6 series of 40 μm coronal brain sections were mounted on slides and air-dried overnight. Slides were stained in 0.05% cresyl fast violet solution with 10% glacial acetic acid for 1 h at 60°C followed by differentiation in 70%, 80%, 90%, 95%, 100% EtOH, 50/50% EtOH/xylene, and 100% xylene. Slides were coverslipped using a xylene-based mountant, DPX.

Visualization of autofluorescent storage material

A 1 in 6 series of 40 μm coronal brain sections was mounted on to Superfrost Plus (Thermo Fisher) slides and air-dried before coverslipping with DAPI (4′,-diamidino-2-phenylindole-dihydrochloride) Fluoromount G (SouthernBiotech).

Immunohistochemistry

A 1 in 6 series of 40 μm coronal brain sections were mounted on slides and briefly air-dried. Slides were blocked in 15% normal goat serum (Vector Laboratories, Burlingame, CA, USA) in Tris-buffered saline (TBS) with Triton-X (Alfa Aesar, Ward Hill, MA, USA) followed by simultaneous incubation in primary antibodies for astrocytes (rabbit polyclonal to GFAP, DAKO cat. no. Z0334, 1:1,000 dilution) and microglia (rat anti-mouse CD68, Bio-Rad, cat. no. MCA1957, 1:400 dilution). Sections were rinsed in TBS and incubated in secondary antibody solution (goat anti-rabbit Alexa Fluor 488, Invitrogen cat. no. A11008, 1:200 dilution and goat anti-rat 546 Alexa Fluor 546, Invitrogen cat. no. A11081, 1:200 dilution). Slides were rinsed and treated with 1× TrueBlack (Biotium, cat. no. 23007) before coverslipping with DAPI Fluoromount-G (SouthernBiotech).

Eyes were embedded in OCT (optimal cutting temperature compound) and stored at −80°C. Horizontal 10 μm sections were cut

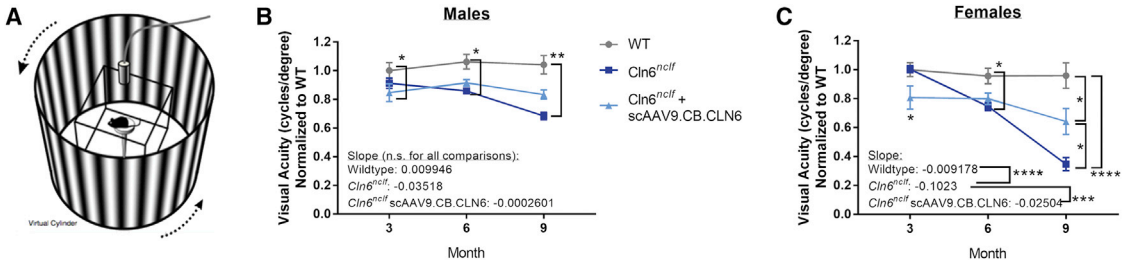

Figure 7. Cerebrospinal fluid delivery of scAAV9.CB.CLN6 partially maintains visual function in *Cln6*^{nclf} mice

(A) Schematic of OptoMotry optokinetic tracking equipment. The test mouse sits on a platform surrounded by four monitors that display a rotating virtual gradient, and the experimenter monitors the animal's visual tracking using an overhead camera. (B and C) A single, postnatal day 1 injection of scAAV9.CB.CLN6 delivered via CSF partially restores visual acuity in male (B) and female (C) *Cln6*^{nclf} mice. When linear fits are compared, untreated female *Cln6*^{nclf} mice have a significantly steeper decline than both female wild-type and AAV9-treated *Cln6*^{nclf} mice (C). Ordinary two-way ANOVA, Tukey correction. For linear fit, slopes were compared using an ordinary one-way ANOVA, Tukey post hoc. Ns are presented in Table 1. Mean ± SEM. *p < 0.05, **p < 0.01, ***p < 0.001, ****p < 0.0001. Image in panel (A) obtained from CerebralMechanics promotional and published materials (http://cerebralmechanics.com/ [23]).

on a cryostat (Leica CM1950), with four sections/slide, and were collected in five series (50 μm apart). One series was stained with cresyl violet for assessing retinal lamination and the other sections were used for immunohistochemistry. Briefly, sections were washed with PBS, blocked in 2% horse serum and 0.3% Triton X-100, and incubated with the following primary antibodies overnight at room temperature: rhodopsin (1:1,000, MAB5356, Millipore), glutamine synthetase (1:1,000, cat. no. 302, Millipore), Brn-3a (1:250, cat. no. sc-31984, Santa Cruz), PKCa (1:250, cat. no. sc-208, Santa Cruz), and human CLN6 (1:250, gift from Stella Lee[8]). Secondary antibodies were goat anti-rabbit Cy3 and goat anti-mouse-Alexa 488. Sections were counterstained with DAPI (Life Technologies). For negative control, sections were treated without primary or secondary antibodies.

RNAscope

Presence of *mCln6* transcript and *hCln6* transcript were visualized in retinal sections by RNAscope using the Multiplex Fluorescent V2 Assay kit (ACDBio cat. no. 323110) in accordance with the manufacturer's protocol. Sections were labeled with either a human *CLN6* probe or a mouse *Cln6* probe (ACDBio), counterstained with DAPI, and mounted on slides using an aqueous mounting medium (Dako Faramount, Agilent).

Imaging and data analysis

Stereological analysis

Estimates of neuron population counts in the DLG nucleus, SC, and V1 were performed using a design-based optical fractionator method in a 1 in 6 series of cresyl fast violet stained sections using Stereo Investigator software (MBF Bioscience).[47] Cells were sampled with counting frames (90 × 100 μm) distributed over a sampling grid (DLG, 300 × 300 μm; SC, 400 × 400 μm; V1, 600 × 600 μm) that was superimposed over the region of interest at 100× magnification.

Thresholding image analysis

Slides for analysis of ASM and immunohistochemistry were scanned using a Zeiss Axio Scan.Z1 (Zeiss, Jena, Germany) at 10× magnification. Scanned images were then analyzed using ImagePro Premier 10 software (Media Cybernetics, Chicago, IL, USA) to manually mark appropriate anatomical regions (DLG, SC, V1) and to select appropriate unique thresholds for individual antibodies and ASM. Thresholds were applied uniformly across all images of a particular region and antibody. Results were reported as percentage positive immunoreactivity (or % fluorescence for ASM).

Retinal sections were examined and images taken using a Leica DM 6000B microscope (Leica Microsystems, Wetzlar, Germany) with Jenoptik camera. Photoreceptors were quantified over a 400 μm length of retina near the optic head, and quantification was performed from 3–5 animals/group. 41 images were obtained from wild-type animals (3–9 months), 25 images from untreated *Cln6*^{nclf} animals, and 31 images from *Cln6*^{nclf} animals + scAAV9.CB.CLN6. Photoreceptors were counted and analyzed using ImageJ threshold and analyze particles functions. The number of photoreceptor layers was gathered from representative images, counting the number of nuclei across the outer nuclear layer. Photoreceptor layer metrics are representative observations, rather than direct quantifications.

CLN6 antibody-stained retinal whole-mounts were evaluated and imaged with an Olympus BX51 Upright Microscope. Twelve images/retina (3 images from central, middle, and peripheral parts of the retina from each quarter, as illustrated in Figure S1) were taken from each retina (n = 3) with fluorescence microscope at 10× magnification. The quantification of fluorescent signals was performed using ImageJ software (NIH) with the threshold and the analyze particles functions.

Optokinetic response

At 3, 6, and 9 months of age, male and female *Cln6*^{nclf} and wild-type mice were placed in an OptoMotry optokinetic tracking chamber (Cerebral Mechanics, http://cerebralmechanics.com/).[23] Briefly, the chamber consisted of four computer monitors facing the animal, displaying a rotating black and white contrast gradient. Blinded experimenters observed whether the animal appeared to see the gradient by intentional head tracking and scored the animal accordingly using

Cerebral Mechanics software. Visual acuity was averaged from both eyes in cycles/degree. n = 11–17 animals/sex at 3 months of age; n = 5–15 animals/sex at 6 months of age; n = 3–11 animals/sex at 9 months of age.

Statistical analysis

Specific statistical tests were calculated using Graphpad Prism and are described in each figure legend. All graphs are represented as mean ± SEM; *p < 0.05, **p < 0.01, ***p < 0.001, ****p < 0.0001.

SUPPLEMENTAL INFORMATION

Supplemental Information can be found online at https://doi.org/10.1016/j.omtm.2020.12.014.

ACKNOWLEDGMENTS

This work was supported through the Charlotte and Gwenyth Gray Foundation and National Institutes of Health (R01NS082283, P20GM103620, and P20GM103548). Slide scanning was performed in part through the use of the Washington University Center for Cellular Imaging (WUCCI) supported by Washington University School of Medicine, the Children's Discovery Institute of Washington University, St. Louis Children's Hospital (CDI-CORE-2015-505 and CDI-CORE-2019-813), and the Foundation for Barnes-Jewish Hospital (3770 and 4642). We would like to thank Dr. Alison Barnwell for helpful comments on the manuscript.

AUTHOR CONTRIBUTIONS

Conceptualization, S.W., J.D.C., and J.M.W.; methodology, S.W., J.D.C., and J.M.W.; validation, K.A.W., H.R.N., T.A.P., B.L., T.B.J., S.D., and A.B.A.; formal analysis, K.A.W., H.R.N., T.A.P., B.L., T.B.J., S.D., and A.B.A.; investigation, K.A.W., H.R.N., T.A.P., B.L., T.B.J., S.D., M.A.P., and A.B.A.; resources, S.L., K.M., and B.K.K.; writing – original draft, K.A.W.; writing – review & editing, K.A.W., H.R.N., J.B., S.W., J.D.C., and J.M.W.; visualization, K.A.W., H.R.N., B.L., M.A.P., S.W., J.D.C., and J.M.W.; supervision, K.A.W., H.R.N., S.W., J.D.C., and J.M.W.; project administration, K.A.W., H.R.N., S.W., J.D.C., and J.M.W.; funding acquisition, S.W., J.D.C., and J.M.W.

DECLARATION OF INTERESTS

The authors declare no competing interests.

REFERENCES

1. Santavuori, P. (1988). Neuronal ceroid-lipofuscinoses in childhood. Brain Dev. *10*, 80–83.
2. Mole, S.E. (2006). Neuronal ceroid lipofuscinoses (NCL). Eur. J. Paediatr. Neurol. *10*, 255–257.
3. Mole, S.E., and Cotman, S.L. (2015). Genetics of the neuronal ceroid lipofuscinoses (Batten disease). Biochim. Biophys. Acta *1852* (10 Pt B), 2237–2241.
4. Cárcel-Trullols, J., Kovács, A.D., and Pearce, D.A. (2015). Cell biology of the NCL proteins: What they do and don't do. Biochim. Biophys. Acta *1852* (10 Pt B), 2242–2255.
5. Johnson, T.B., Cain, J.T., White, K.A., Ramirez-Montealegre, D., Pearce, D.A., and Weimer, J.M. (2019). Therapeutic landscape for Batten disease: current treatments and future prospects. Nat. Rev. Neurol. *15*, 161–178.
6. Lewis, G., Morrill, A.M., Conway-Allen, S.L., and Kim, B. (2020). Review of Cerliponase Alfa: Recombinant Human Enzyme Replacement Therapy for Late-Infantile Neuronal Ceroid Lipofuscinosis Type 2. J. Child Neurol. *35*, 348–353.
7. Schulz, A., Ajayi, T., Specchio, N., de Los Reyes, E., Gissen, P., Ballon, D., Dyke, J.P., Cahan, H., Slasor, P., Jacoby, D., and Kohlschütter, A.; CLN2 Study Group (2018). Study of Intraventricular Cerliponase Alfa for CLN2 Disease. N. Engl. J. Med. *378*, 1898–1907.
8. Cain, J.T., Likhite, S., White, K.A., Timm, D.J., Davis, S.S., Johnson, T.B., Dennys-Rivers, C.N., Rinaldi, F., Motti, D., Corcoran, S., et al. (2019). Gene Therapy Corrects Brain and Behavioral Pathologies in CLN6-Batten Disease. Mol. Ther *27*, 1836–1847.
9. Kleine Holthaus, S.M., Herranz-Martin, S., Massaro, G., Aristorena, M., Hoke, J., Hughes, M.P., Maswood, R., Semenyuk, O., Basche, M., Shah, A.Z., et al. (2019). Neonatal brain-directed gene therapy rescues a mouse model of neurodegenerative CLN6 Batten disease. Hum. Mol. Genet. *28*, 3867–3879.
10. AmicusTherapeutics (2019). Positive Interim Clinical Data from Ongoing Phase 1/2 Study in CLN6 Batten Disease (Amicus), https://ir.amicusrx.com/events/event-details/amicus-therapeutics-presents-positive-interim-clinical-data-cln6-batten.
11. Lundstrom, K. (2018). Viral Vectors in Gene Therapy. Diseases *6*, 42.
12. Weinberg, M.S., Samulski, R.J., and McCown, T.J. (2013). Adeno-associated virus (AAV) gene therapy for neurological disease. Neuropharmacology *69*, 82–88.
13. DiCarlo, J.E., Mahajan, V.B., and Tsang, S.H. (2018). Gene therapy and genome surgery in the retina. J. Clin. Invest. *128*, 2177–2188.
14. Hammond, S.L., Leek, A.N., Richman, E.H., and Tjalkens, R.B. (2017). Cellular selectivity of AAV serotypes for gene delivery in neurons and astrocytes by neonatal intracerebroventricular injection. PLoS ONE *12*, e0188830.
15. Aguirre, G.D. (2017). Concepts and Strategies in Retinal Gene Therapy. Invest. Ophthalmol. Vis. Sci. *58*, 5399–5411.
16. Bosch, M.E., Aldrich, A., Fallet, R., Odvody, J., Burkovetskaya, M., Schuberth, K., Fitzgerald, J.A., Foust, K.D., and Kielian, T. (2016). Self-Complementary AAV9 Gene Delivery Partially Corrects Pathology Associated with Juvenile Neuronal Ceroid Lipofuscinosis (CLN3). J. Neurosci. *36*, 9669–9682.
17. Meyer, K., Ferraiuolo, L., Schmelzer, L., Braun, L., McGovern, V., Likhite, S., Michels, O., Govoni, A., Fitzgerald, J., Morales, P., et al. (2015). Improving single injection CSF delivery of AAV9-mediated gene therapy for SMA: a dose-response study in mice and nonhuman primates. Mol. Ther. *23*, 477–487.
18. Hinderer, C., Katz, N., Buza, E.L., Dyer, C., Goode, T., Bell, P., Richman, L.K., and Wilson, J.M. (2018). Severe Toxicity in Nonhuman Primates and Piglets Following High-Dose Intravenous Administration of an Adeno-Associated Virus Vector Expressing Human SMN. Hum. Gene Ther. *29*, 285–298.
19. Kremkow, J., and Alonso, J.M. (2018). Thalamocortical Circuits and Functional Architecture. Annu. Rev. Vis. Sci. *4*, 263–285.
20. Weimer, J.M., Custer, A.W., Benedict, J.W., Alexander, N.A., Kingsley, E., Federoff, H.J., Cooper, J.D., and Pearce, D.A. (2006). Visual deficits in a mouse model of Batten disease are the result of optic nerve degeneration and loss of dorsal lateral geniculate thalamic neurons. Neurobiol. Dis. *22*, 284–293.
21. Ito, S., and Feldheim, D.A. (2018). The Mouse Superior Colliculus: An Emerging Model for Studying Circuit Formation and Function. Front. Neural Circuits *12*, 10.
22. Watanabe, S., Sanuki, R., Ueno, S., Koyasu, T., Hasegawa, T., and Furukawa, T. (2013). Tropisms of AAV for subretinal delivery to the neonatal mouse retina and its application for in vivo rescue of developmental photoreceptor disorders. PLoS ONE *8*, e54146.
23. Douglas, R.M., Alam, N.M., Silver, B.D., McGill, T.J., Tschetter, W.W., and Prusky, G.T. (2005). Independent visual threshold measurements in the two eyes of freely moving rats and mice using a virtual-reality optokinetic system. Vis. Neurosci. *22*, 677–684.
24. Kielar, C., Maddox, L., Bible, E., Pontikis, C.C., Macauley, S.L., Griffey, M.A., Wong, M., Sands, M.S., and Cooper, J.D. (2007). Successive neuron loss in the thalamus and cortex in a mouse model of infantile neuronal ceroid lipofuscinosis. Neurobiol. Dis. *25*, 150–162.

25. Pontikis, C.C., Cotman, S.L., MacDonald, M.E., and Cooper, J.D. (2005). Thalamocortical neuron loss and localized astrocytosis in the Cln3Deltaex7/8 knock-in mouse model of Batten disease. Neurobiol. Dis. *20*, 823–836.

26. Morgan, J.P., Magee, H., Wong, A., Nelson, T., Koch, B., Cooper, J.D., and Weimer, J.M. (2013). A murine model of variant late infantile ceroid lipofuscinosis recapitulates behavioral and pathological phenotypes of human disease. PLoS ONE *8*, e78694.

27. Mathieu, E., Gupta, N., Ahari, A., Zhou, X., Hanna, J., and Yücel, Y.H. (2017). Evidence for Cerebrospinal Fluid Entry Into the Optic Nerve via a Glymphatic Pathway. Invest. Ophthalmol. Vis. Sci. *58*, 4784–4791.

28. Kleine Holthaus, S.M., Ribeiro, J., Abelleira-Hervas, L., Pearson, R.A., Duran, Y., Georgiadis, A., Sampson, R.D., Rizzi, M., Hoke, J., Maswood, R., et al. (2018). Prevention of Photoreceptor Cell Loss in a $Cln6^{nclf}$ Mouse Model of Batten Disease Requires CLN6 Gene Transfer to Bipolar Cells. Mol. Ther. *26*, 1343–1353.

29. Griffey, M., Macauley, S.L., Ogilvie, J.M., and Sands, M.S. (2005). AAV2-mediated ocular gene therapy for infantile neuronal ceroid lipofuscinosis. Mol. Ther. *12*, 413–421.

30. Whiting, R.E.H., Robinson Kick, G., Ota-Kuroki, J., Lim, S., Castaner, L.J., Jensen, C.A., Kowal, J., Nguyen, A., Corado, C., O'Neill, C.A., and Katz, M.L. (2020). Intravitreal enzyme replacement inhibits progression of retinal degeneration in canine CLN2 neuronal ceroid lipofuscinosis. Exp. Eye Res. *198*, 108135.

31. Bartsch, S., Liu, J., Bassal, M., Jankowiak, W., Spitzer, M.S., and Bartsch, U. (2020). Experimental therapeutic approaches for the treatment of retinal dystrophy in neuronal ceroid lipofuscinosis. Ophthalmologe. Published online October 8, 2020. https://doi.org/10.1007/s00347-020-01237-9.

32. Kleine Holthaus, S.M., Aristorena, M., Maswood, R., Semenyuk, O., Hoke, J., Hare, A., Smith, A.J., Mole, S.E., and Ali, R.R. (2020). Gene Therapy Targeting the Inner Retina Rescues the Retinal Phenotype in a Mouse Model of CLN3 Batten Disease. Hum. Gene Ther. *31*, 709–718.

33. Lang, J.F., Toulmin, S.A., Brida, K.L., Eisenlohr, L.C., and Davidson, B.L. (2019). Standard screening methods underreport AAV-mediated transduction and gene editing. Nat. Commun. *10*, 3415.

34. Wang, J., Xie, J., Lu, H., Chen, L., Hauck, B., Samulski, R.J., and Xiao, W. (2007). Existence of transient functional double-stranded DNA intermediates during recombinant AAV transduction. Proc. Natl. Acad. Sci. USA *104*, 13104–13109.

35. Khabou, H., Cordeau, C., Pacot, L., Fisson, S., and Dalkara, D. (2018). Dosage Thresholds and Influence of Transgene Cassette in Adeno-Associated Virus-Related Toxicity. Hum. Gene Ther. *29*, 1235–1241.

36. Reichel, F.F., Dauletbekov, D.L., Klein, R., Peters, T., Ochakovski, G.A., Seitz, I.P., Wilhelm, B., Ueffing, M., Biel, M., Wissinger, B., et al.; RD-CURE Consortium (2017). AAV8 Can Induce Innate and Adaptive Immune Response in the Primate Eye. Mol. Ther. *25*, 2648–2660.

37. Xiong, W., Wu, D.M., Xue, Y., Wang, S.K., Chung, M.J., Ji, X., Rana, P., Zhao, S.R., Mai, S., and Cepko, C.L. (2019). AAV *cis*-regulatory sequences are correlated with ocular toxicity. Proc. Natl. Acad. Sci. USA *116*, 5785–5794.

38. Katz, M.L., Tecedor, L., Chen, Y., Williamson, B.G., Lysenko, E., Wininger, F.A., Young, W.M., Johnson, G.C., Whiting, R.E., Coates, J.R., and Davidson, B.L. (2015). AAV gene transfer delays disease onset in a TPP1-deficient canine model of the late infantile form of Batten disease. Sci. Transl. Med. *7*, 313ra180.

39. Bohlen, M.O., McCown, T.J., Powell, S.K., El-Nahal, H.G., Daw, T., Basso, M.A., Sommer, M.A., and Samulski, R.J. (2020). Adeno-Associated Virus Capsid-Promoter Interactions in the Brain Translate from Rat to the Nonhuman Primate. Hum. Gene Ther. *31*, 1155–1168.

40. Lee, S.H., Yang, J.Y., Madrakhimov, S., Park, H.Y., Park, K., and Park, T.K. (2018). Adeno-Associated Viral Vector 2 and 9 Transduction Is Enhanced in Streptozotocin-Induced Diabetic Mouse Retina. Mol. Ther. Methods Clin. Dev. *13*, 55–66.

41. Green, F., Samaranch, L., Zhang, H.S., Manning-Bog, A., Meyer, K., Forsayeth, J., and Bankiewicz, K.S. (2016). Axonal transport of AAV9 in nonhuman primate brain. Gene Ther. *23*, 520–526.

42. Castle, M.J., Gershenson, Z.T., Giles, A.R., Holzbaur, E.L., and Wolfe, J.H. (2014). Adeno-associated virus serotypes 1, 8, and 9 share conserved mechanisms for anterograde and retrograde axonal transport. Hum. Gene Ther. *25*, 705–720.

43. Hennig, A.K., Levy, B., Ogilvie, J.M., Vogler, C.A., Galvin, N., Bassnett, S., and Sands, M.S. (2003). Intravitreal gene therapy reduces lysosomal storage in specific areas of the CNS in mucopolysaccharidosis VII mice. J. Neurosci. *23*, 3302–3307.

44. Yu-Wai-Man, P., Newman, N.J., Carelli, V., Moster, M.L., Biousse, V., Sadun, A.A., Klopstock, T., Vignal-Clermont, C., Sergott, R.C., Rudolph, G., et al. (2020). Bilateral visual improvement with unilateral gene therapy injection for Leber hereditary optic neuropathy. Sci. Transl. Med. *12*, eaaz7423.

45. Bible, E., Gupta, P., Hofmann, S.L., and Cooper, J.D. (2004). Regional and cellular neuropathology in the palmitoyl protein thioesterase-1 null mutant mouse model of infantile neuronal ceroid lipofuscinosis. Neurobiol. Dis. *16*, 346–359.

46. Groh, J., Kühl, T.G., Ip, C.W., Nelvagal, H.R., Sri, S., Duckett, S., Mirza, M., Langmann, T., Cooper, J.D., and Martini, R. (2013). Immune cells perturb axons and impair neuronal survival in a mouse model of infantile neuronal ceroid lipofuscinosis. Brain *136*, 1083–1101.

47. West, M.J., Slomianka, L., and Gundersen, H.J. (1991). Unbiased stereological estimation of the total number of neurons in thesubdivisions of the rat hippocampus using the optical fractionator. Anat. Rec. *231*, 482–497.